



ARL-TR-8022 • MAY 2017



US Army Research Laboratory

Compression-after-Impact and Bend Fatigue Results of Glass/Epoxy Composites with Compliant Interlayer and Needling Interlaminar Enhancements

by Robert A Haynes, Steven E Boyd, and Bradley D Lawrence

Approved for public release; distribution is unlimited.

NOTICES

Disclaimers

The findings in this report are not to be construed as an official Department of the Army position unless so designated by other authorized documents.

Citation of manufacturer's or trade names does not constitute an official endorsement or approval of the use thereof.

Destroy this report when it is no longer needed. Do not return it to the originator.



Compression-after-Impact and Bend Fatigue Results of Glass/Epoxy Composites with Compliant Interlayer and Needling Interlaminar Enhancements

by Robert A Haynes

Vehicle and Technology Directorate, ARL

Steven E Boyd

Weapons and Materials Research Directorate, ARL

Bradley D Lawrence

Bennett Aerospace, Inc., Cary, NC

REPORT DOCUMENTATION PAGE				Form Approved OMB No. 0704-0188	
<p>Public reporting burden for this collection of information is estimated to average 1 hour per response, including the time for reviewing instructions, searching existing data sources, gathering and maintaining the data needed, and completing and reviewing the collection information. Send comments regarding this burden estimate or any other aspect of this collection of information, including suggestions for reducing the burden, to Department of Defense, Washington Headquarters Services, Directorate for Information Operations and Reports (0704-0188), 1215 Jefferson Davis Highway, Suite 1204, Arlington, VA 22202-4302. Respondents should be aware that notwithstanding any other provision of law, no person shall be subject to any penalty for failing to comply with a collection of information if it does not display a currently valid OMB control number.</p> <p>PLEASE DO NOT RETURN YOUR FORM TO THE ABOVE ADDRESS.</p>					
1. REPORT DATE (DD-MM-YYYY) May 2017		2. REPORT TYPE Technical Report		3. DATES COVERED (From - To) 1 October 2013–30 September 2016	
4. TITLE AND SUBTITLE Compression-after-Impact and Bend Fatigue Results of Glass/Epoxy Composites with Compliant Interlayer and Needling Interlaminar Enhancements				5a. CONTRACT NUMBER	
				5b. GRANT NUMBER	
				5c. PROGRAM ELEMENT NUMBER	
6. AUTHOR(S) Robert A Haynes, Steven E Boyd, and Bradley D Lawrence				5d. PROJECT NUMBER	
				5e. TASK NUMBER	
				5f. WORK UNIT NUMBER	
7. PERFORMING ORGANIZATION NAME(S) AND ADDRESS(ES) US Army Research Laboratory ATTN: RDRL-VTM Aberdeen Proving Ground, MD 21005-5066				8. PERFORMING ORGANIZATION REPORT NUMBER ARL-TR-8022	
9. SPONSORING/MONITORING AGENCY NAME(S) AND ADDRESS(ES)				10. SPONSOR/MONITOR'S ACRONYM(S)	
				11. SPONSOR/MONITOR'S REPORT NUMBER(S)	
12. DISTRIBUTION/AVAILABILITY STATEMENT Approved for public release; distribution is unlimited.					
13. SUPPLEMENTARY NOTES					
14. ABSTRACT In this work, we tested 2-D and 3-D woven S2-glass/SC-15 epoxy composite laminates with compliant interlayer and needling interlaminar enhancements for single impact performance, compression-after-impact strength, and bend and shear fatigue life. The interlaminar enhancements decreased the strength and stiffness of the material but improved the durability. Needling had a larger improvement in compression-after-impact strength than the compliant interlayer, while the compliant interlayer had a larger improvement in stress-versus-fatigue-life slope than the needling.					
15. SUBJECT TERMS composite materials, interlaminar enhancement, durability, damage tolerance, compliant interlayer					
16. SECURITY CLASSIFICATION OF:			17. LIMITATION OF ABSTRACT UU	18. NUMBER OF PAGES 32	19a. NAME OF RESPONSIBLE PERSON Robert A Haynes
a. REPORT Unclassified	b. ABSTRACT Unclassified	c. THIS PAGE Unclassified			19b. TELEPHONE NUMBER (Include area code) 410-278-2397

Contents

List of Figures	iv
List of Tables	v
Acknowledgments	vi
1. Introduction	1
2. Interlaminar Enhancement Technologies	1
2.1 Compliant Interlayer	2
2.2 Needling	3
3. Test Plan	3
4. Results	6
4.1 Impact Response and Compression after Impact	6
4.2 3-Point Bend	14
4.3 Short-Beam Shear	18
5. Conclusions and Recommendations	19
6. References	20
List of Symbols, Abbreviations, and Acronyms	23
Distribution List	24

List of Figures

Fig. 1	Representative 3-point bend test setup	2
Fig. 2	Low-velocity impact of 2-D woven fabric panels displacement response with various interlaminar enhancements	7
Fig. 3	Low-velocity impact of 2-D woven fabric panels energy response with various interlaminar enhancements.....	7
Fig. 4	Low-velocity impact of 2-D woven fabric panels response with various interlaminar enhancements.....	8
Fig. 5	Low-velocity impact of 2-D woven fabric panels force response with various interlaminar enhancements.....	8
Fig. 6	Low-velocity impact of 2-D woven fabric panels velocity response with various interlaminar enhancements	9
Fig. 7	CAI residual compressive strength after low-velocity impact of 2-D woven fabric panels with various interlaminar enhancements	9
Fig. 8	Low-velocity impact displacement response for 3-D TPU interlayer composites.....	10
Fig. 9	Low-velocity measured impact energy for 3-D TPU interlayer composites.....	11
Fig. 10	Low-velocity impact response for 3-D TPU interlayer composites ...	11
Fig. 11	Ultrasonic c-scan images of single low-velocity impact damage for the 3-D T.E.A.M. baseline panels (top row), the 5-mil TPU panels (middle row), and the 10-mil TPU panels (bottom row). Individual specimens have alphabetic designations A–F.	12
Fig. 12	Ultrasonic c-scan images of single low-velocity impact damage for the 3-D T.E.A.M. hybrid panels containing 10-mil TPU (top row) and 20-mil TPU (bottom row). Individual specimens have numeric designations; the 10-mil panel only had 5 specimens in sample group.	12
Fig. 13	3-point bend maximum stress vs. fatigue life for panels A–C.....	16
Fig. 14	3-point bend maximum stress vs. fatigue life for panels D–F	16
Fig. 15	3-point bend maximum stress vs. fatigue life for panels G–J.....	17
Fig. 16	3-point bend maximum stress vs. fatigue life for panels K–M.....	17
Fig. 17	Short-beam shear maximum stress vs. fatigue life for panels D–F	18

List of Tables

Table 1	Test matrix and sample dimensions (length [cm] × width [cm] × thickness [cm]) for evaluation of compliant interlayer (CI) and needling interlaminar enhancement techniques in 2-D woven glass fabrics.....	4
Table 2	List of material constituents, geometries, densities for the 3-D composite materials	6
Table 3	3-D T.E.A.M. composite panel data from impact and compression after impact testing with damage area analysis.....	13
Table 4	Static bend strength for 3-point bend tests of 2-D woven fabric panels	15
Table 5	Modulus with coefficient of variation (CoV) and slope of the stress vs. fatigue life (S-N) curve for 3-point bend tests of 2-D woven fabric panels	15
Table 6	Strength and modulus from high-speed, static, and 3-point bend tests of 2-D woven fabric panels.....	18
Table 7	Static shear strength and modulus with coefficient of variation (CoV) and slope of the stress vs. fatigue life (S-N) curve for short-beam shear tests of 2-D woven fabric panels.....	19

Acknowledgments

The authors would like to thank Mr Jim Wolbert, Mr Mike Neblett, Mr Mike Thompson, Mr Fred Racine, and Mr Rob Miller for panel processing and sample preparation. The authors would also like to thank Mr Jordan Wagner and Mr Art Yiournas for conducting the ultrasonic scanning, and Mr Albert Tran for assisting with the fatigue testing.

1. Introduction

Composite materials are gaining popularity in structural applications because of their high in-plane specific strength and stiffness; however, composites traditionally have poor out-of-plane (i.e., interlaminar or through-the-thickness) properties.¹ Compression-after-impact (CAI) strength is often a driver of composite material allowables.² Further, structural materials subject to repeated loading and unloading will degrade (i.e., fatigue); interlaminar damage growth is an important driver of fatigue life in composite materials.³ Improving the interlaminar durability and damage tolerance could produce a material with more desirable allowables without changing the fiber or matrix.

Many interlaminar enhancement technologies have been tried and can be categorized into 2 main groups: inserting reinforcement through the thickness spanning multiple plies, and adding a durable or damage-tolerant layer between plies. Braiding, flocking, pultrusion, stitching, tufting, weaving, and z-pinning are types of through-the-thickness reinforcement that have been evaluated.⁴ The National Aeronautics and Space Administration has had success with its Pultruded Rod Stitched Efficient Unitized Structure (PRSEUS),⁵ demonstrating that the enhancement allowed the structure to carry loads 52% above the requirement, even when subject to impact damage. Often thermoplastic sheets are used in interlayer-toughened composites.⁶ Shivakumar and Panduranga⁷ have reviewed thermoplastic interleaving methods and note improvements in the interlaminar fracture toughness of nearly 400% in some cases. Many existing interlaminar enhancement technologies are expensive to fabricate; the methods presented in this work use relatively inexpensive materials and are relatively simple to manufacture.

This work was in support of the Army's Durable Hybrid Composites and Extremely Lightweight, Adaptive, Durable, and Damage Tolerant (XLADD) structures programs.

2. Interlaminar Enhancement Technologies

In this work, 2 interlaminar enhancement technologies (compliant interlayer and needling) for composite materials are evaluated for their improvement of the CAI strength and fatigue life of 2-D and 3-D woven glass fabrics. For the 2-D fabrics, the base laminate to which the enhancements are applied is [0]₈ composed of a 24 oz/yd² woven roving S2-glass/SC-15 epoxy material system.^{8,9} This is a relatively thin laminate as compared to other investigations with these interlaminar enhancement technologies. The interlayer is inserted at the midplane, and the

needling is performed to each of two $[0]_4$ sublaminates. A 3-D weave S2-glass laminate and a hybrid laminate with a Kevlar layer are also investigated. The 3-D weave fabric is composed of Owens Corning Shieldstrand S-glass (warp, weft, and z-weaver fibers) and woven by T.E.A.M.^{10,11} The Kevlar layer is a 2-D woven style 386 from Hexcel.¹² For the 3-D laminates, the thermoplastic polyurethane (TPU) film interlayer is also inserted between the outer 3-D weave layers at the midplane. For the hybrid laminate, 2 TPU film interlayers are used with the woven Kevlar placed at the midplane. CAI, quasi-static and fatigue 3-point bend, and quasi-static and fatigue short-beam shear testing are performed on select configurations.

2.1 Compliant Interlayer

The compliant interlayer consists of a thin film of thermoplastic ester-based polyurethane adhesive polymer (UAF-472)¹³ located between sublaminates of the larger laminate (Fig. 1). Two thicknesses were evaluated for the 2-D materials: 0.13 and 0.25 mm (5 and 10 mil), located at the midplane of the laminate. For the 3-D materials, 2 thicknesses of TPU film were evaluated: 0.25 and 0.51 mm (10 and 20 mil). To produce the panels for this work, during manufacturing the film is placed between mats prior to a vacuum-assisted resin transfer molding (VARTM) process followed by curing.^{14,15}

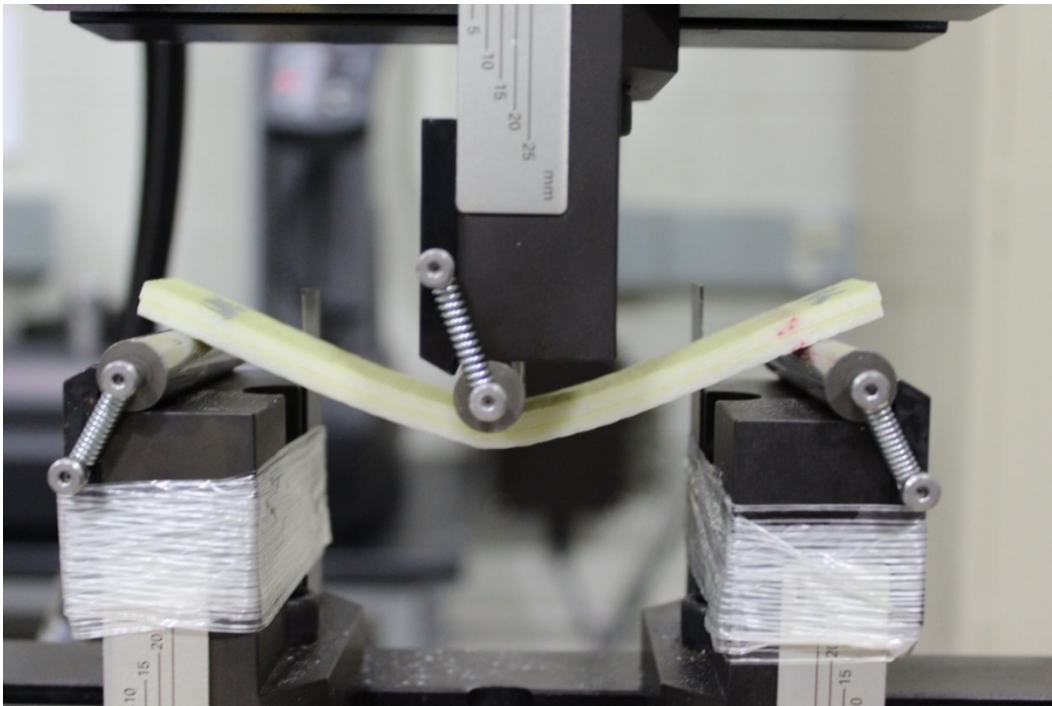


Fig. 1 Representative 3-point bend test setup

The benefit of the compliant interlayer is believed to be its ability to undergo large deformation, particularly shear, without fracturing. This leads to a partial decoupling of the sublaminates on either side of the compliant interlayer. When a laminate with a compliant interlayer experiences significant bending, such as when impacted on its face, it has been shown that there will be larger out-of-plane deflection but less delamination than if the laminate did not have the compliant interlayer.¹⁶

2.2 Needling

Needling consists of pushing nominally 12.4-mm (0.500-inch) short aramid fibers through plies of in-plane fibers.¹⁷ These short fibers are initially randomly oriented in a mat, which is laid on top of the laminate; barbed needles designed to catch only a few fibers at a time push through the mat and plies, depositing the short fibers as z-fiber bundles. The areal density of punctures can be controlled through the needling process by modulating the feed rate and stitching pattern geometry. In this work aramid fibers are needled through 4 plies of the woven glass fibers with a perforation density of 85 perforations/cm² to create a sublaminate. One laminate was needled in error at a higher perforation areal density (greater than 100 perforations/cm²); the cured laminate was included in the test regimen. To produce panels for this work, 2 needled sublaminates were stacked prior to a VARTM process followed by curing.¹⁷ Three control panels having a nominally identical layup with the mat of aramid fiber but with 0 perforations/cm² were fabricated and tested as well.

The benefit of needling is believed to be its ability to provide reinforcement between individual plies such that when interlaminar tension or shear is experienced, the reinforcement will carry the load and prevent the formation and spread of delamination. Improvements in Modes I and II fracture toughness have been demonstrated.¹⁸

3. Test Plan

For the 2-D materials, 13 panels were fabricated with combinations of the 2 interlaminar enhancement technologies included and subject to CAI, 3-point bend, and short-beam shear tests. The tests complemented other durability and damage tolerance testing that was performed under the same program^{17,18}; the bend and shear tests were chosen specifically to create high shear stresses at the midplane where the compliant interlayer was located. Table 1 presents the laminate configurations fabricated and tests performed. Panels A–C were manufactured earlier than panels D–J, and to ensure consistency, panels D–F duplicate the configuration of panels A–C.

Table 1 Test matrix and sample dimensions (length [cm] × width [cm] × thickness [cm]) for evaluation of compliant interlayer (CI) and needling interlaminar enhancement techniques in 2-D woven glass fabrics

Panel label	CI	Needling	CAI (cm)	3PB (cm)	SBS (cm)
A	None	None	NA	15.2 × 2.53 × 0.640	NA
B	5 mil	None	NA	15.2 × 2.53 × 0.663	NA
C	10 mil	None	NA	15.2 × 2.54 × 0.675	NA
D	None	None	15.1 × 10.1 × 0.546	15.2 × 2.45 × 0.534	7.60 × 1.14 × 0.530
E	5 mil	None	15.1 × 10.1 × 0.559	15.2 × 2.46 × 0.559	7.60 × 1.15 × 0.545
F	10 mil	None	15.1 × 10.1 × 0.569	15.2 × 2.47 × 0.562	7.60 × 1.15 × 0.558
G	None	85 perfs/cm ²	15.1 × 10.1 × 0.632	15.2 × 2.46 × 0.630	NA
H	5 mil	85 perfs/cm ²	15.1 × 10.1 × 0.663	15.2 × 2.47 × 0.663	NA
I	10 mil	85 perfs/cm ²	15.1 × 10.1 × 0.670	15.2 × 2.45 × 0.665	NA
J	None	>100 perfs/cm ²	15.1 × 10.2 × 0.721	15.2 × 2.47 × 0.723	NA
K	None	Control	NA	15.2 × 2.58 × 0.698	NA
L	5 mil	Control	NA	15.2 × 2.59 × 0.746	NA
M	10 mil	Control	NA	15.2 × 2.59 × 0.772	NA

Notes: Tests included compression-after-impact (CAI), 3-point bend (3PB), and short-beam shear (SBS); NA indicates testing not performed.

Sample dimensions are provided in Table 1. As expected, inclusion of the compliant interlayer and the needling-induced Z-fiber architecture produce thicker laminates. Low-velocity impact performance was determined through testing per ASTM D 7136,¹⁹ and CAI strength was measured per ASTM D 7137.²⁰

Three-point bend testing was conducted using ASTM D 7264²¹ as a guide. The supports and loading nose diameters were 1.27 cm (0.500 inch), and the span of the supports was nominally 12.7 cm (5.00 inches); the span-to-thickness ratio was approximately 20 inches this work; see Fig. 1 for a representative test setup. For all panels, 6–8 specimens were tested in quasi-static monotonic loading to determine the strength. Testing was conducted at 4.06 mm/min (0.160 inch/min). Four additional specimens each from Panels A–C were tested at higher rates: 2 at 406 mm/min (16 inches/min) and 2 at 8130 mm/min (320 inches/min); this was to investigate rate sensitivity of the compliant interlayer. Four samples from each panel with 6–8 specimens in each sample were subject to fatigue at 2 Hz and an R-ratio of 0.1, with each sample experiencing a maximum load of 90%, 80%, 70%, and 60% of the ultimate strength, respectively.






Short-beam shear testing was conducted on panels D–F using ASTM D 2344²² as a guide. The supports and loading nose diameters were 3.18 mm (0.125 inch), and the span of the supports was nominally 2.54 cm (1.00 inch); the span-to-thickness ratio was approximately 4 inches in this work. Six specimens were tested in quasi-static monotonic loading to determine the strength. Testing was conducted at 4.06 mm/min (0.160 inch/min). Four samples from each panel with 6 specimens in each sample

were subject to fatigue at 2 Hz and an R-ratio of 0.1, with each sample experiencing a maximum load of 90%, 80%, 70%, and 60% of the ultimate strength, respectively.

Because of improvements in impact performance and durability observed in thick-section composites,^{14,15} the testing methodology presented for the 2-D materials was also extended to 3-D weave fabric materials. Three composite panels with the T.E.A.M. S-glass weave were manufactured; a baseline panel containing no TPU film interlayers and a 5- and 10-mil TPU panel. The panels were specifically manufactured to evaluate the effect of the TPU film interlayer and its thickness on impact and postimpact properties. Though no 3-D fabrics were needed, 2 hybrid panels were manufactured to include a 2-D woven layer of Hexcel Kevlar 49 with 2 interlayers of 10- and 20-mil TPU. The Kevlar layer was included in an attempt to combine the tear and punching shear resistance of Kevlar with the decoupling effect of the TPU interlayers with the overall aim of improving the impact durability of the composite. There is no corresponding 3-D T.E.A.M. hybrid panel with no TPU because of processing issues encountered with dry spots and voids during infusion.

All 3-D panels were tested for single low-velocity impact performance per ASTM D 7136¹⁹ and for CAI strength per ASTM D 7137.²⁰ The lay-ups were specifically designed to place the interlaminar enhancement (either TPU film or combination of TPU film and Kevlar) at the midplane and to manufacture panels with an approximate areal density of 10 kg/m² (2 psf). The impact and CAI panels were cut using a waterjet to nominal dimensions of 101.6 × 152.4 mm (4.00 × 6.00 inches) according to ASTM D 7136; the loading surfaces were then machined flat using a diamond-coated machine tool for maximum uniformity and to minimize damage to the sample. Table 2 gives the composite material panel dimensions, lay-up, and areal densities. After the panels were impacted and before CAI testing, the panels were ultrasonically scanned to produce a c-scan image of the damage area from the single impact. The damage area was analyzed digitally with ImageJ²³ and reported. No 3-point bending or short-beam shear testing was performed on the 3-D composite materials.

Table 2 List of material constituents, geometries, densities for the 3-D composite materials

Composite (SC-15 Resin)	Lay-up	Thickness (mm)	Areal density kg/m ² (lb/ft ²)
3-D T.E.A.M. (no TPU)		6.2	10.5 (2.14)
3-D T.E.A.M. + 5-mil TPU		6.6	11.0 (2.25)
3-D T.E.A.M. + 10-mil TPU		6.8	11.2 (2.28)
3-D T.E.A.M. + 10-mil TPU + Kevlar		7.9	...
3-D T.E.A.M. + 20-mil TPU + Kevlar		8.4	13.4 (2.7)

4. Results

The results are categorized by test: CAI, 3-point bend, and short-beam shear.

4.1 Impact Response and Compression after Impact

The results for the impact testing of the panels with 2-D woven glass fabrics are provided in Figs. 2–6 for displacement versus time, energy versus time, force versus displacement, force versus time, and velocity versus time, respectively. Of particular note are the larger forces and smaller displacements experienced by the overneedled specimens. A comparison of CAI strength for all panels is provided in Fig. 7. Inclusion of a compliant interlayer alone improved the strength by up to 13% as compared to the baseline. Inclusion of needling alone improved the strength by 21%. Inclusion of both technologies improved the strength by up to 43%. Overneedling improved the strength by 73%.

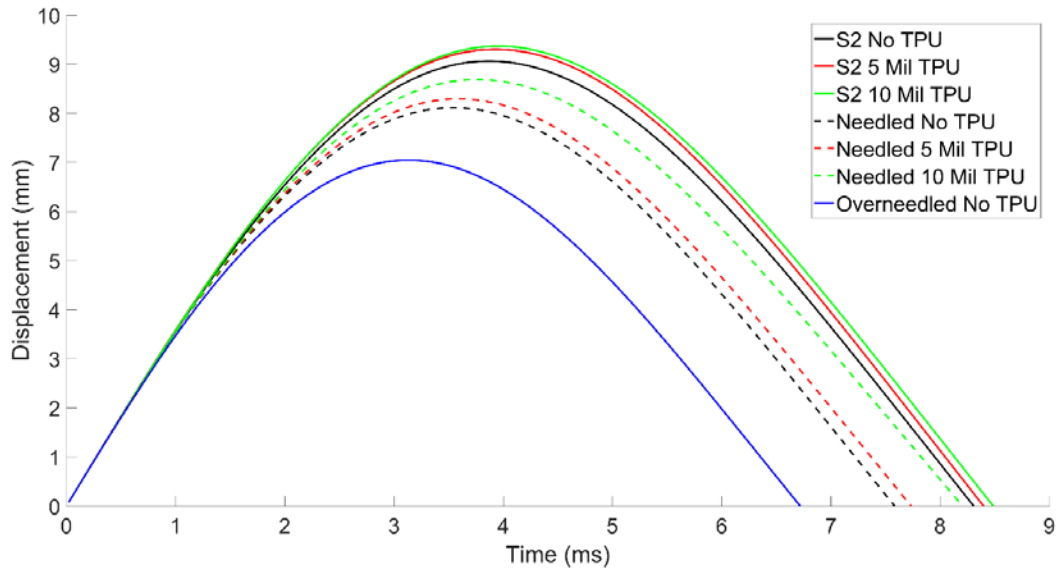


Fig. 2 Low-velocity impact of 2-D woven fabric panels displacement response with various interlaminar enhancements

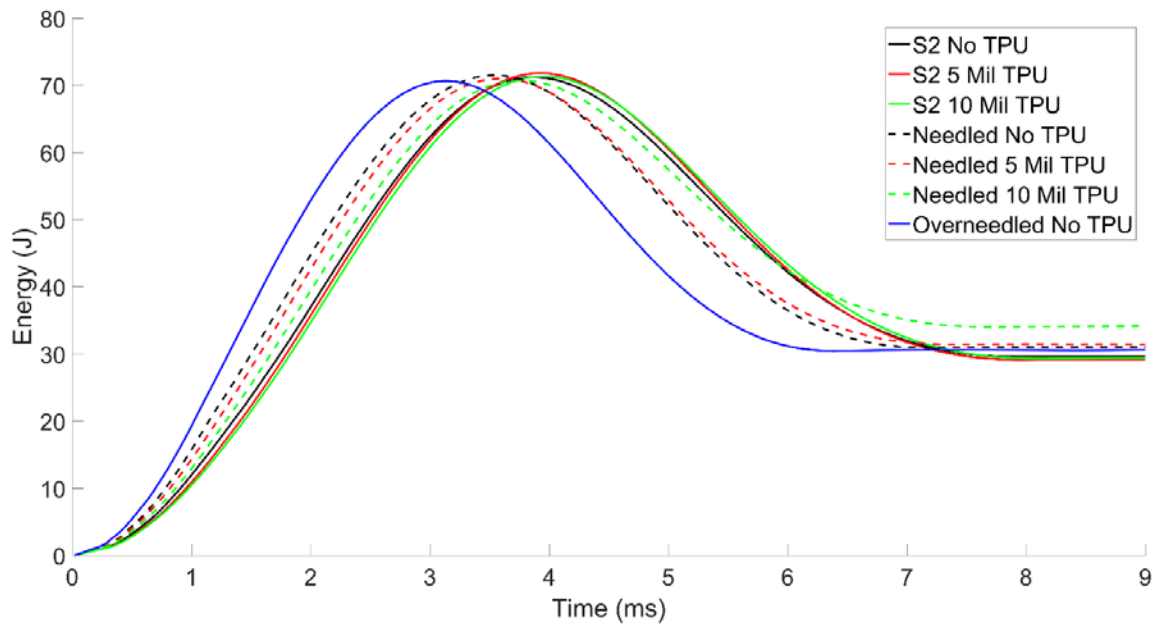


Fig. 3 Low-velocity impact of 2-D woven fabric panels energy response with various interlaminar enhancements

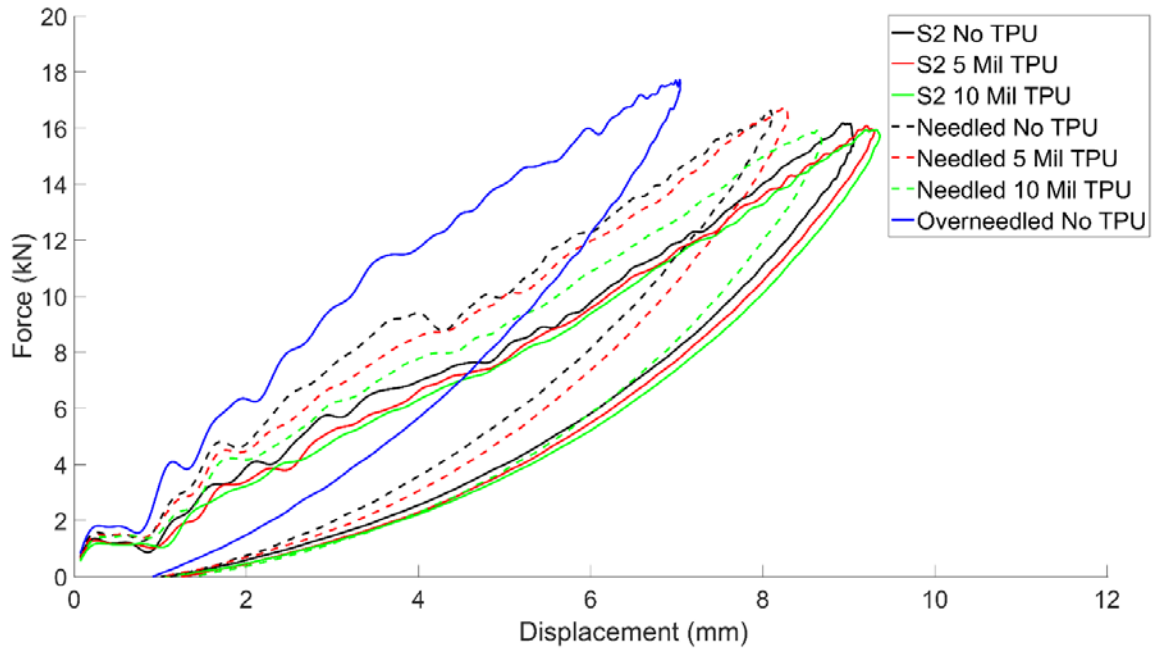


Fig. 4 Low-velocity impact of 2-D woven fabric panels response with various interlaminar enhancements

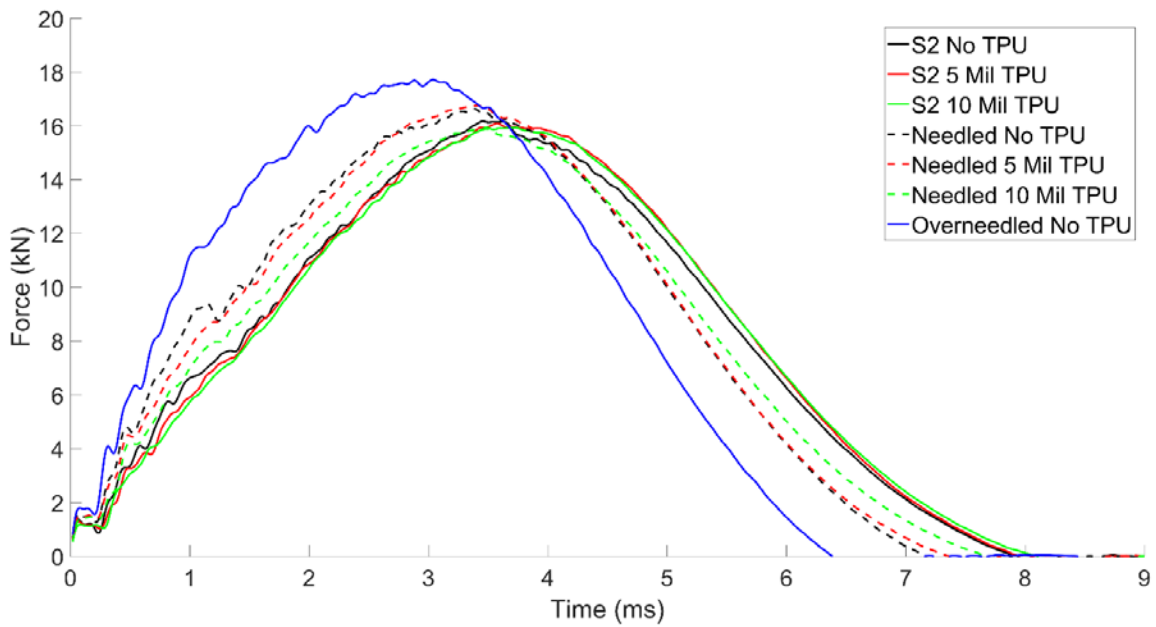


Fig. 5 Low-velocity impact of 2-D woven fabric panels force response with various interlaminar enhancements

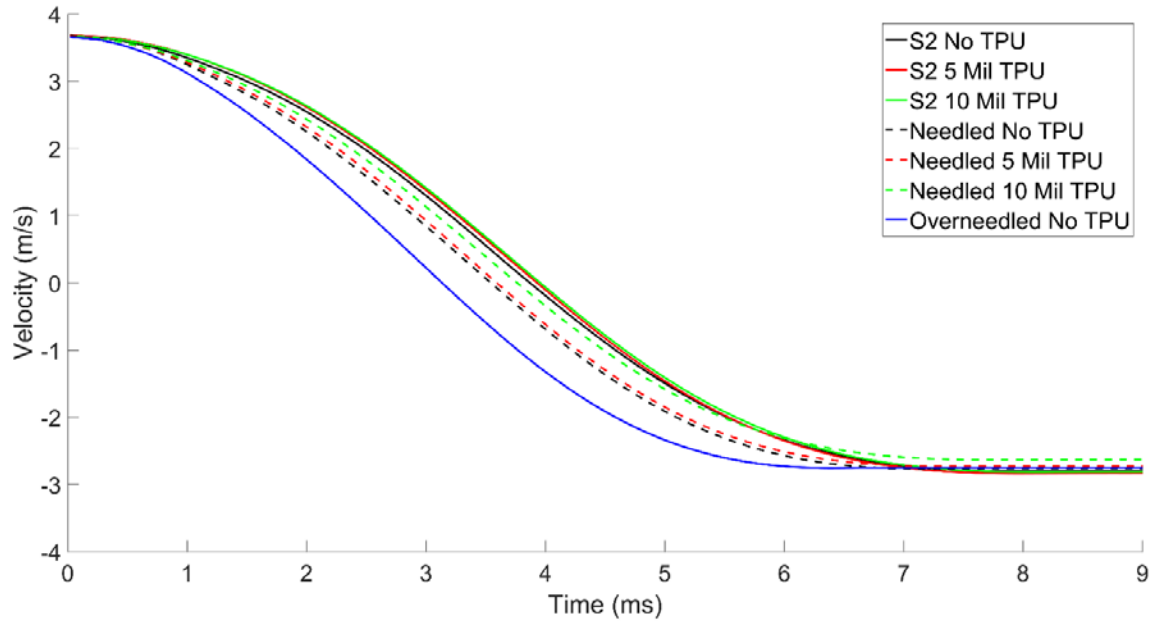


Fig. 6 Low-velocity impact of 2-D woven fabric panels velocity response with various interlaminar enhancements

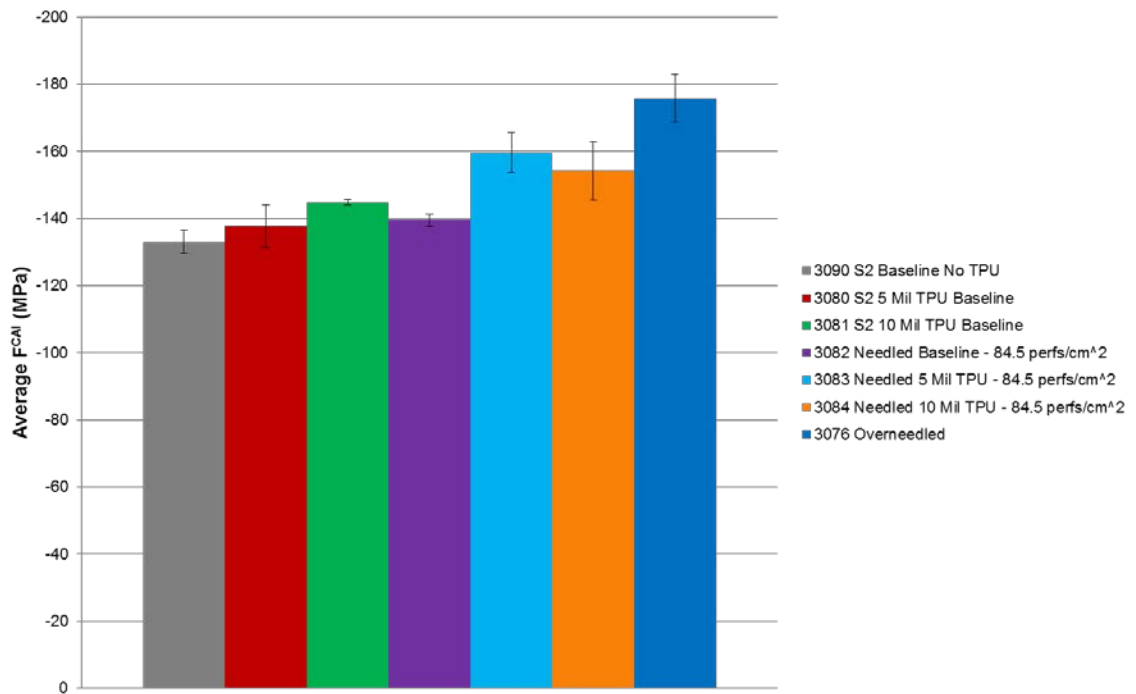


Fig. 7 CAI residual compressive strength after low-velocity impact of 2-D woven fabric panels with various interlaminar enhancements

The single low-velocity impacts on the 3-D panels are represented in Figs. 8–12. Panel displacement (deflection calculated from Eqs. 9 and 10 in ASTM D 7136¹⁹) versus time is plotted in Fig. 8. The impact energy (measured energy given in Eq. 5 in ASTM D 7136¹⁹) versus time is plotted in Fig. 9. Finally, the measured impact force profile (measured from the impact tup) is plotted versus the displacement given in Fig. 8 to yield the force-deflection impact curve of Fig. 10. Relevant data values for impact, damage assessment, and CAI strength are stated in Table 3. Ultrasonic c-scans of the 3-D panels are presented in Figs. 11 and 12 for the nonhybrid 3-D T.E.A.M. panels and the hybrid panels, respectively.

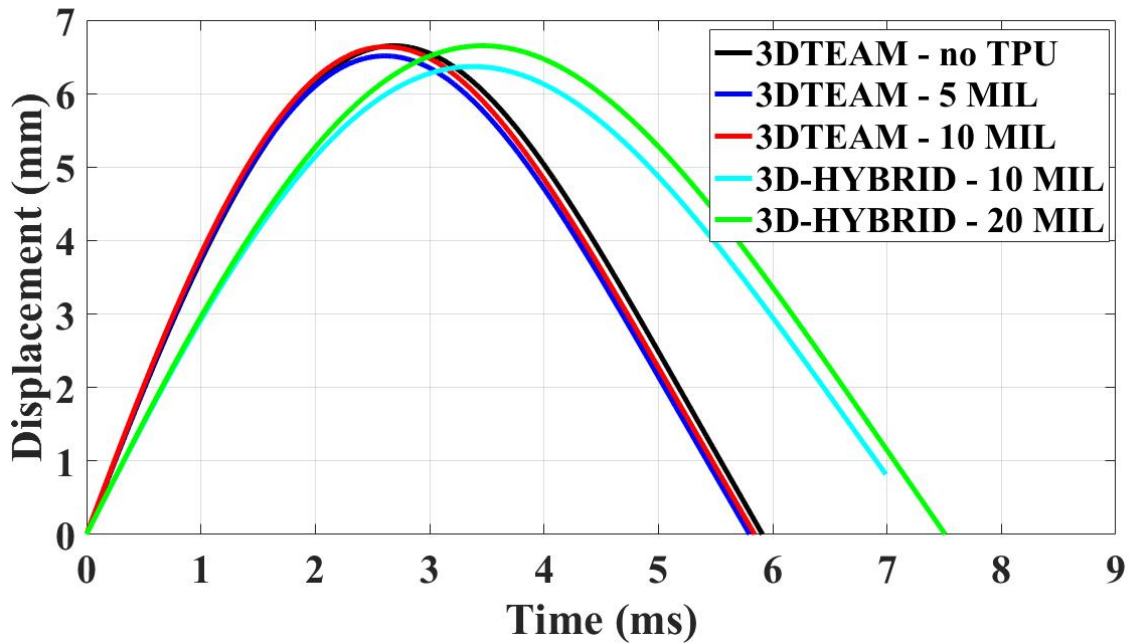


Fig. 8 Low-velocity impact displacement response for 3-D TPU interlayer composites

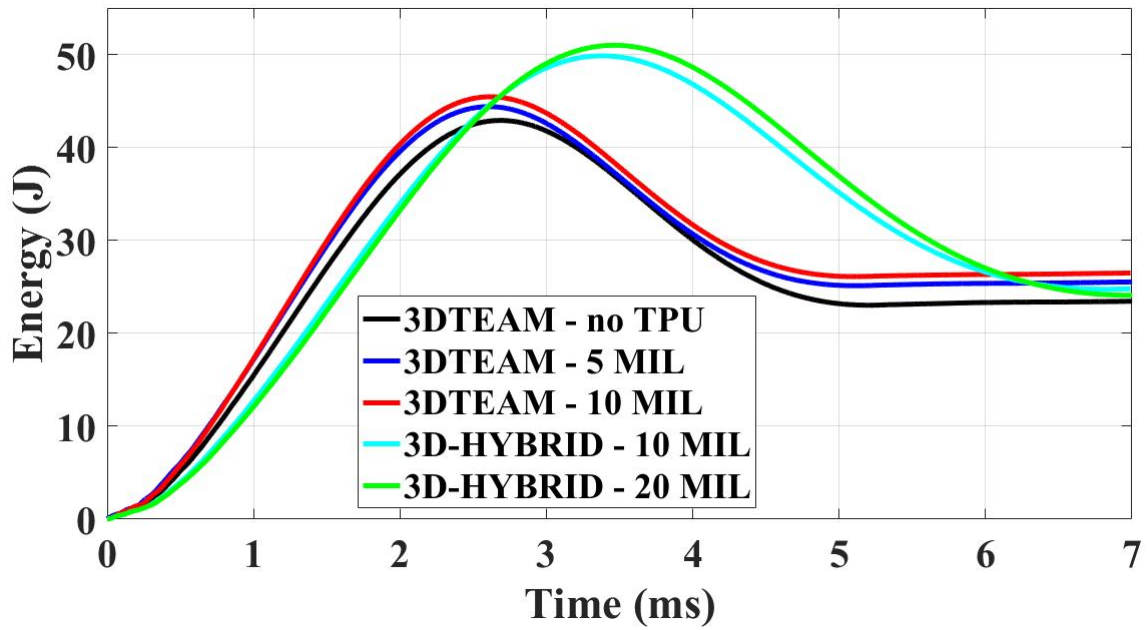


Fig. 9 Low-velocity measured impact energy for 3-D TPU interlayer composites

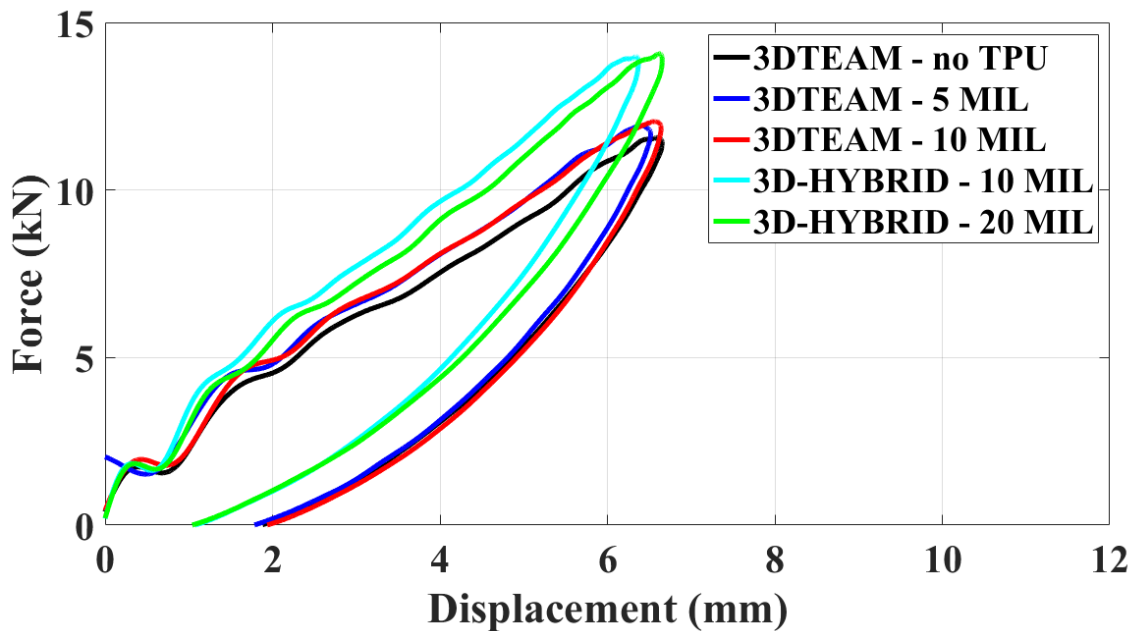


Fig. 10 Low-velocity impact response for 3-D TPU interlayer composites

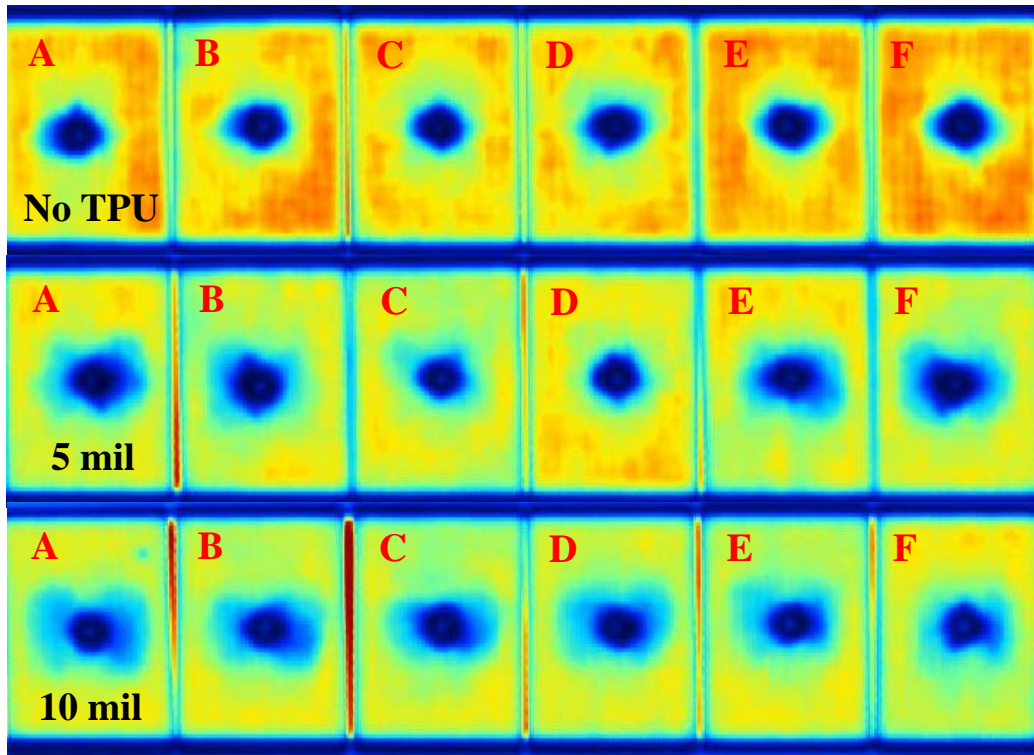


Fig. 11 Ultrasonic c-scan images of single low-velocity impact damage for the 3-D T.E.A.M. baseline panels (top row), the 5-mil TPU panels (middle row), and the 10-mil TPU panels (bottom row). Individual specimens have alphabetic designations A-F.

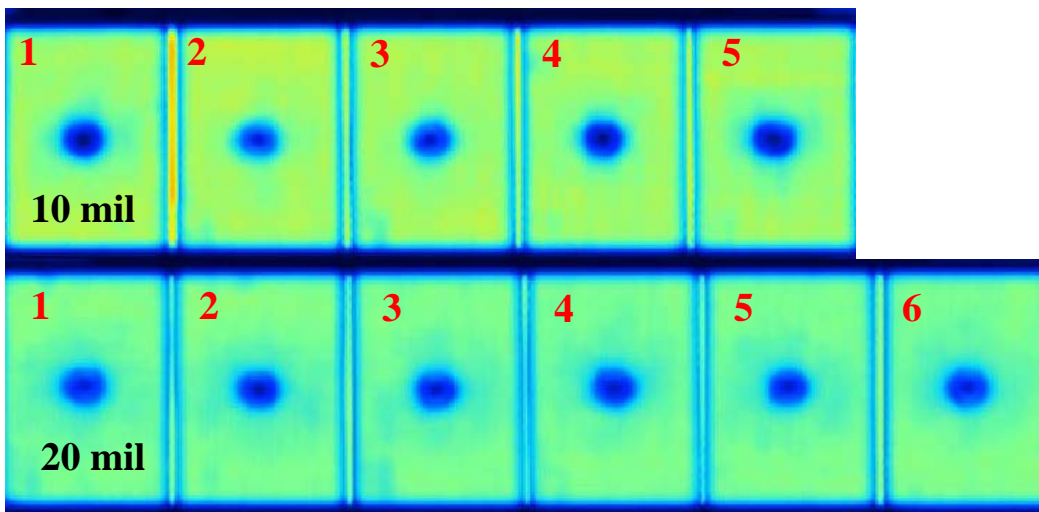


Fig. 12 Ultrasonic c-scan images of single low-velocity impact damage for the 3-D T.E.A.M. hybrid panels containing 10-mil TPU (top row) and 20-mil TPU (bottom row). Individual specimens have numeric designations; the 10-mil panel only had 5 specimens in sample group.

Table 3 3-D T.E.A.M. composite panel data from impact and compression after impact testing with damage area analysis

Composite (SC-15 Resin)	Single impact ASTM 7136		Damage area (% of aperture)	CAI strength ASTM 7137 (MPa)
	Peak load (kN)	Peak displacement (mm)		
3-D T.E.A.M. (no TPU)	11.7 ± 0.11	6.65 ± 0.05	9.6 ± 1.1	154.7 ± 6.8
3-D T.E.A.M. + 5-mil TPU	11.7 ± 0.74	6.28 ± 0.29	11.6 ± 2.7	157.4 ± 7.0
3-D T.E.A.M. + 10-mil TPU	12.1 ± 0.13	6.64 ± 0.12	11.1 ± 1.0	158.9 ± 5.8
3-D T.E.A.M. + 10-mil TPU + Kevlar	14.0 ± 0.16	6.35 ± 0.15	5.9 ± 0.6	149.4 ± 9.0
3-D T.E.A.M. + 20-mil TPU + Kevlar	14.1 ± 0.25	6.61 ± 0.20	6.6 ± 0.6	137.1 ± 1.5

In Figs. 8–10 and Table 3, there is little distinction between the baseline, 5-mil, and 10-mil panels in the impact data. All samples have similar peak loads and deflections, CAI strengths, and damage areas. One notable difference is the damage areas revealed on the c-scans of Fig. 11 and Table 3. The 3-D T.E.A.M. baseline panel has 2% less damage area per aperture (the cut-out area of the impact support in ASTM D 7136¹⁹) than both TPU interlayer panels. The 3-D T.E.A.M. panels with 5- and 10-mil TPU seem to have a “halo” of damage surrounding the immediate dark blue damage under the impactor. This effect was observed for thick-section composites and is known to be an area of matrix cracking due to the compliant TPU interlayer allowing the composite sublayers to decouple and allow more flexure under the impact, as determined through sectioning and microscopy. The damage area of the baseline panel is less because the damage is more localized matrix cracking, fiber crushing, delamination, and, perhaps, fiber punching under the impactor. From Fig. 9, the impact energy of the 3-D T.E.A.M. baseline, 5-mil, and 10-mil TPU panels was approximately 44 J, which is consistent with ASTM D 7136.¹⁹ Increasing the impact energy may provide a stronger delineation between impact response of the baseline, 5-mil, and 10-mil panels.

The 3-D T.E.A.M. hybrid panels with 10- and 20-mil TPU were impacted at 50 J according to ASTM D 7136.¹⁹ Figure 8 and Table 3 show that the 20-mil TPU panel deflects to 6.6 mm, 4% more under impact than the 10-mil panel, although both have similar peak loads. From the force-deflection response of Fig. 10, the impact

stiffness (kN/cm) of the hybrid, the 20-mil sample is noticeably less than the 10-mil panel, with a decrease of 14% at 1-cm deflection. The damage area for the hybrid 20-mil panel is approximately 1% greater as determined by digital image analysis from Figs. 11 and 12. These data are consistent with the fact that adding twice the thickness of compliant TPU film at the midplane of the composite will result in more compliance, greater deflection, and increased impact damage due to that deflection. The CAI strength is also diminished by 8% as stated in Table 3.

The 2-D Kevlar layer has a distinct effect on the impact response of the 3-D T.E.A.M. composites, as demonstrated in Figs. 8–10 and Table 3. The key difference can be seen in the damage areas and the CAI strengths. The hybrid composites sustained a 20% larger impact energy, yet both the hybrid 10 and 20-mil TPU panels had smaller damage areas as compared to the group. The hybrid 10-mil TPU panel had a 47% drop in damage area over the 3-D T.E.A.M. 10-mil TPU panel. The CAI strengths were noticeably lower overall with the 2-D Kevlar layer. The hybrid 10-mil TPU composite had a 6% drop in CAI strength. The addition of the 2-D Kevlar layer improves composite durability under impact but compromises in-plane mechanical properties.

4.2 3-Point Bend

The average static flexural strengths and moduli of the specimens from each panel are provided in Tables 4 and 5, respectively, along with the percent change relative to Panel D, which was the baseline with no interlaminar enhancement techniques applied. Panels A–C had an approximately 10% lower strength than Panels D–F, possibly due to manufacturing variations. With just needling, the strength and modulus dropped by 22% and 14%, respectively. The compliant interlayer alone performed slightly better than the needling alone. In general, the 5-mil interlayer performed slightly better than the 10-mil interlayer, but having both needling and an interlayer performed worse than one interlaminar enhancement technique alone. The predominant failure mode was compression under the loading nose.

Table 4 Static bend strength for 3-point bend tests of 2-D woven fabric panels

Panel label	CI	Needling	Strength (MPa)	CoV (%)	Change from baseline
A	None	None	404	4.5	...
B	5 mil	None	355	9.9	...
C	10 mil	None	365	5.7	...
D	None	None	461	4.2	Baseline
E	5 mil	None	400	6.1	-13.2%
F	10 mil	None	389	3.5	-15.6%
G	None	Standard	359	19	-22.1%
H	5 mil	Standard	362	7.3	-21.5%
I	10 mil	Standard	332	5.4	-28.0%
J	None	Over	396	2.9	-14.1%
K	None	Control	400	2.4	-13.2%
L	5 mil	Control	326	2.4	-29.3%
M	10 mil	Control	414	5.0	-10.2%

Note: CI = compliant interlayer, and CoV = coefficient of variation.

Table 5 Modulus with coefficient of variation (CoV) and slope of the stress vs. fatigue life (S-N) curve for 3-point bend tests of 2-D woven fabric panels

Panel label	CI	Needling	Modulus (GPa)	CoV (%)	Change from baseline	Slope of the S-N curve (MPa/log _e cycles)
A	None	None	17.9	3.0	...	-18.0
B	5 mil	None	16.3	2.2	...	-15.0
C	10 mil	None	16.6	5.2	...	-17.3
D	None	None	21.5	3.1	Baseline	-19.1
E	5 mil	None	19.5	4.4	-9.30	-17.3
F	10 mil	None	16.8	5.4	-21.9	-16.0
G	None	Standard	18.5	2.3	-14.0	-19.7
H	5 mil	Standard	14.7	8.6	-31.6	-14.2
I	10 mil	Standard	10.5	16	-51.2	-17.1
J	None	Over	15.2	1.5	-29.3	-14.9
K	None	Control	9.25	1.7	-57.0	-20.4
L	5 mil	Control	11.7	2.7	-45.6	-37.4
M	10 mil	Control	13.0	2.8	-39.5	-15.4

Stress-fatigue life curves are provided in Figs. 13–17. The slope of the stress-fatigue life curve can be considered to be a measure of durability, where the slope is found from a linear regression between the maximum stress and the natural log of the number of cycles to failure; the slopes are provided in Table 5. With the exception of the control samples, all samples incorporating a compliant interlayer exhibited a higher durability by 10%–20% than samples without a compliant interlayer; on average 5-mil samples performed 6.8% better than 10-mil samples. With the exception of the control and overneedled samples, the needled samples were within 3% of the nonneedled panels. Again, with the exception of the control samples, the overneedled sample exhibited a 21% higher durability than the other

samples without a compliant interlayer. The control samples exhibited a 43% worse durability on average than the noncontrol samples. The predominant failure mode was compression under the loading nose.

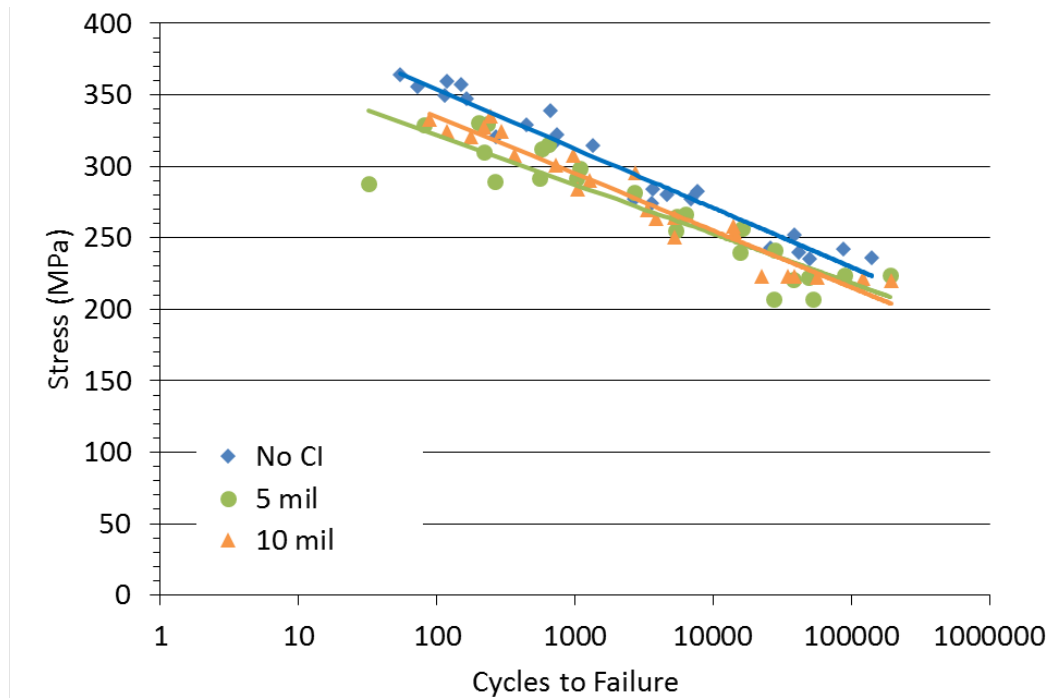


Fig. 13 3-point bend maximum stress vs. fatigue life for panels A–C

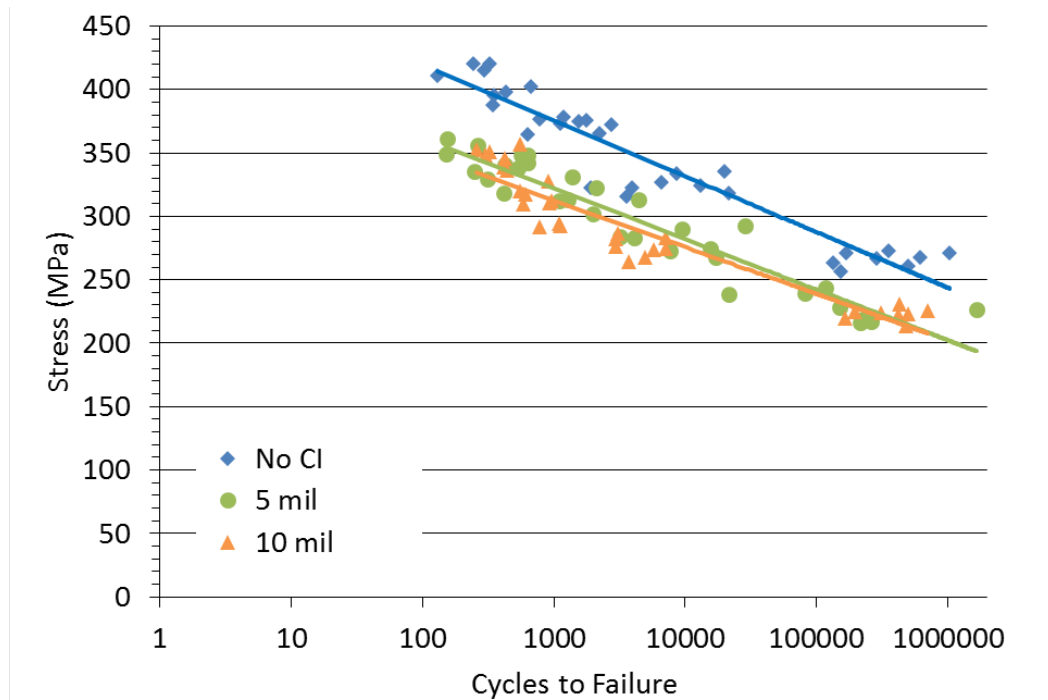


Fig. 14 3-point bend maximum stress vs. fatigue life for panels D–F

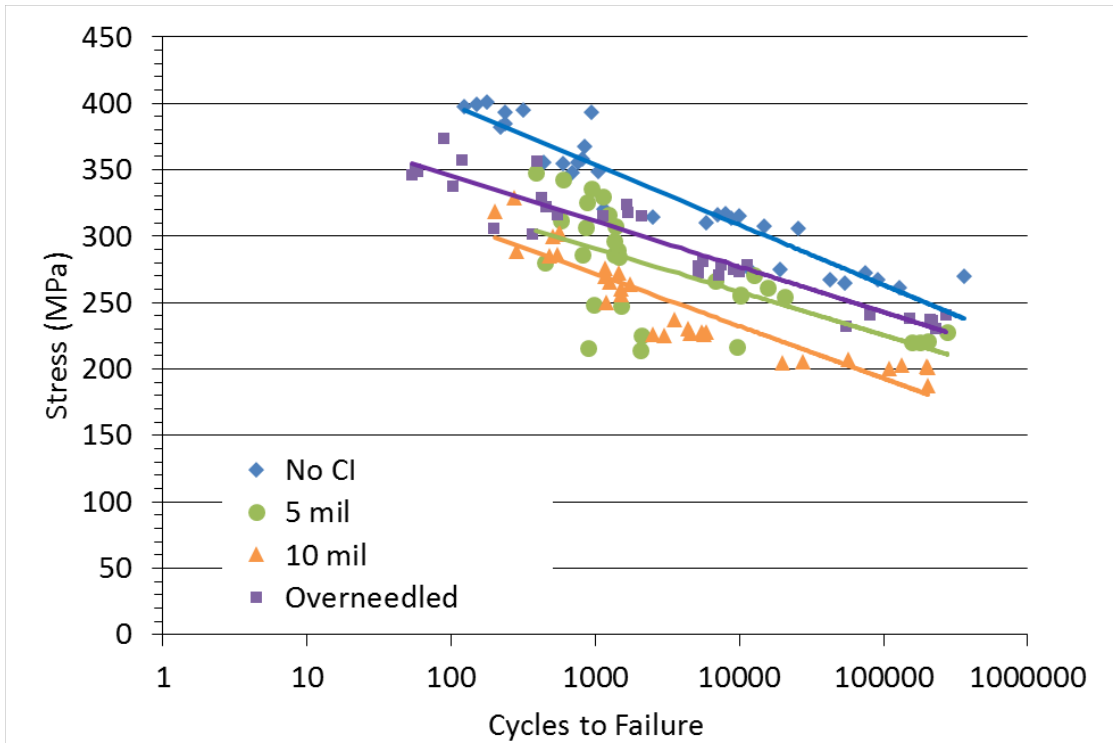


Fig. 15 3-point bend maximum stress vs. fatigue life for panels G–J

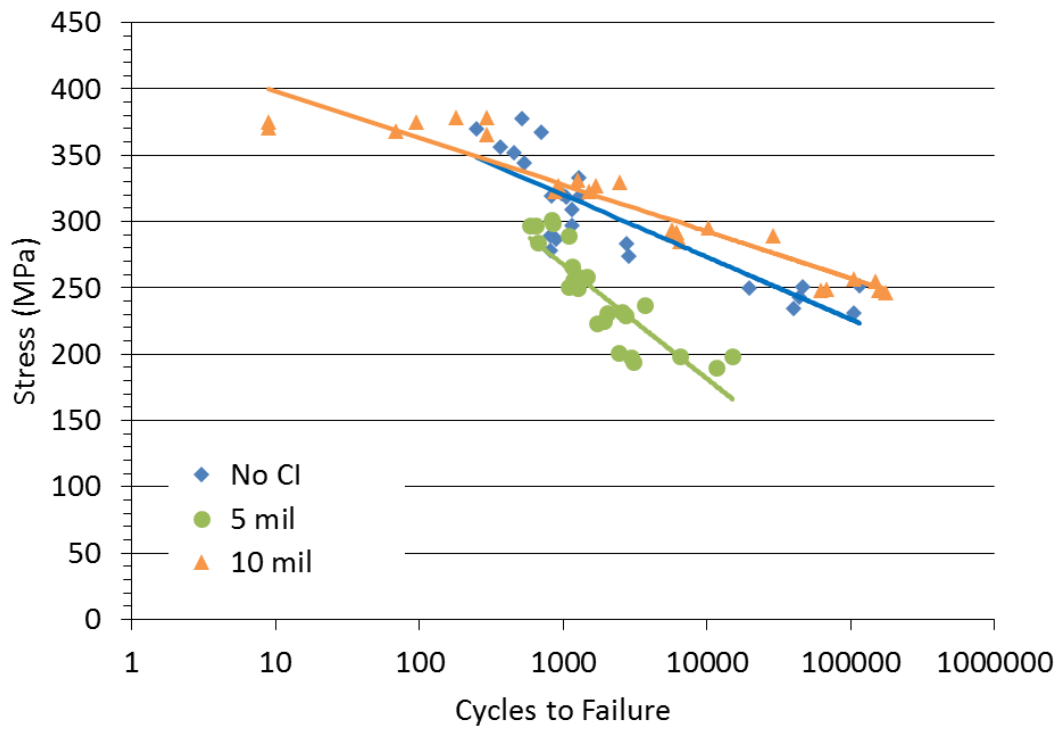


Fig. 16 3-point bend maximum stress vs. fatigue life for panels K–M

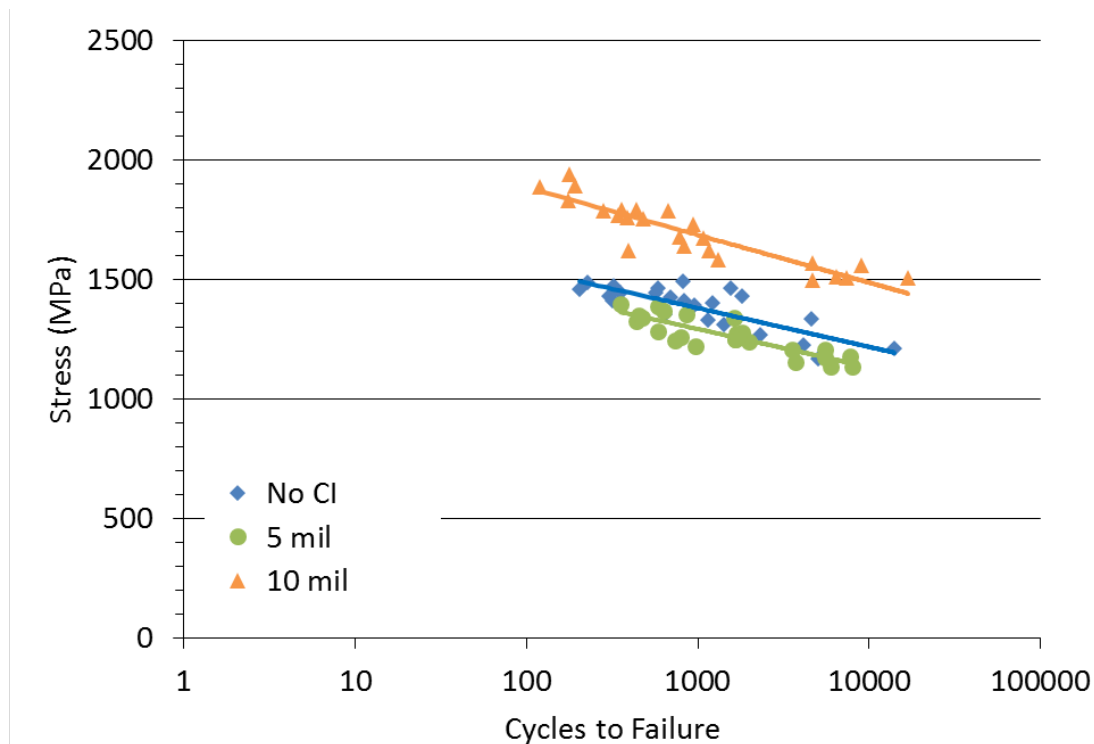


Fig. 17 Short-beam shear maximum stress vs. fatigue life for panels D–F

The high-speed static test results are provided in Table 6. A 14% increase in the strength was observed in the 16 inches/min samples over the 0.16 inches/min samples, suggesting a rate dependency, but there was a negligible difference in strength between the 16 and 320 inches/min samples. A negligible difference in modulus was seen between the 0.16 and 16 inches/min samples, whereas a 6.9% increase in modulus was seen between the 0.16 and 320 inches/min samples.

Table 6 Strength and modulus from high-speed, static, and 3-point bend tests of 2-D woven fabric panels

Panel label	CI	Needling	16 inches/min		320 inches/min	
			Strength (MPa)	Modulus (GPa)	Strength (MPa)	Modulus (GPa)
A	None	None	422	18.7	459	19.0
B	5 mil	None	426	16.9	415	17.8
C	10 mil	None	424	16.3	420	17.5

4.3 Short-Beam Shear

The average static shear strengths and moduli of each panel are provided in Table 7. The 5- and 10-mil compliant interlayer samples exhibited a 7.7% decrease and an 18% increase in strength, respectively, as compared to the sample without a compliant interlayer. Figure 17 shows the stress versus fatigue life plots for the 3

panels tested in short-beam shear; the slopes of the curve fits are provided in Table 7. The 5- and 10-mil compliant interlayer samples exhibited a 1.7% increase and a 23% decrease in durability, respectively, as compared to the sample without a compliant interlayer.

Table 7 Static shear strength and modulus with coefficient of variation (CoV) and slope of the stress vs. fatigue life (S-N) curve for short-beam shear tests of 2-D woven fabric panels

Panel label	CI	Needling	Strength (MPa)	CoV (%)	Modulus (GPa)	CoV (%)	Slope of the S-N curve (MPa/log _e cycles)
D	None	None	72.8	4.0	4.07	9.3	-70.5
E	5 mil	None	67.2	4.7	3.72	4.4	-69.3
F	10 mil	None	85.8	3.6	5.87	4.3	-86.7

5. Conclusions and Recommendations

All interlaminar enhancement technologies improved the CAI strength and decreased the 3-point bend strength and modulus for the 2-D composites. The overneedled sample appeared to have the best overall properties; it had the best CAI strength, one of the highest retained 3-point bend strengths, and one of the lowest stress-versus-fatigue-life slopes. It is recommended that this technology be investigated further. Adding a compliant interlayer generally resulted in higher durability, although the results were mixed between the 2 thicknesses. Needling had a larger improvement in CAI strength than the compliant interlayer, while the compliant interlayer had a larger improvement in stress-versus-fatigue-life slope than the needling. Slight increases in strength and stiffness were observed when testing at higher rates, indicating the presence of some form of rate dependency for these composite architectures.

Adding TPU films to the 3-D T.E.A.M. composites was inconclusive, possibly because of the use of a relatively low impact energy level (44 J) pursuant to ASTM D 7136.¹⁹ Doubling the energy for these single impact tests may better elucidate the benefits of adding TPU films on impact durability through interlaminar toughening. An improvement in the impact response and durability was demonstrated by adding a 2-D woven Kevlar layer, but with a corresponding reduction in in-plane CAI strength. The results indicate that for all composites manufactured with TPU film interlayers, adding thicker TPU films results in a more compliant and thicker composite panel.

6. References

1. O'Brien TK. Composite interlaminar shear fracture toughness, G_{IIC} : shear measurements or sheer myth? Bucinell RB, editor. West Conshohocken (PA): American Society for Testing and Materials; 1998. p. 3–18. (Composite materials: fatigue and fracture; vol. 7, ASTM STP 1300).
2. Hodge AJ, Nettles AT, Jackson JR. Comparison of open-hole compression strength and compression after impact strength on carbon fiber/epoxy laminates for the Ares I composite interstage. Huntsville (AL): National Aeronautics and Space Administration; 2011 Mar. Report No.: NASA/TP-2011-216460.
3. Talreja R. Fatigue of composite materials. Lancaster (PA): Technomic Pub. Co.; 1987.
4. Ranatunga V, Clay S. Study of delamination onset under mode-II loading in translaminar reinforced composites using acoustic emission techniques. Dayton (OH): American Society for Composites; 2014.
5. Lovejoy A, Rouse M, Linton K, Li V. Pressure testing of a minimum gauge PRSEUS panel. 52nd AIAA/ASME/ASCE/AHS/ASC Structures, Structural Dynamics and Materials Conference, Structures, Structural Dynamics, and Materials and Co-located conferences; 2011 Apr 4–7; Denver, CO.
6. Hayes B, Gammon L. Optical microscopy of fiber-reinforced composites. Novelty (OH): ASM International; 2010.
7. Shivakumar K, Panduranga R. Interleaved polymer matrix composites - a review. 54th AIAA/ASME/ASCE/AHS/ASC Structures, Structural Dynamics, and Materials Conference. 2013 Apr 8–11; Boston, MA.
8. S2-glass. Aiken (SC): AGY; c2017 [accessed 2017 May 2]. <http://www.agy.com/products/s-glass/>.
9. SC-15 resin. Benicia (CA): Applied Poleramic Inc.; c2017 [accessed 2017 May 2]. <http://www.appliedpoleramic.com/>.
10. ShieldStrand woven fabrics. Toledo (OH): Owens Corning Composite Materials, LLC; 2010 Jan [accessed 2017 May 2]. http://www.ocvreinforcements.com/pdf/products/ShieldStrand_S_Fabrics.pdf.
11. Style 0015-02. Woonsocket (RI): Textile Engineering and Manufacturing (T.E.A.M.); nd [accessed 2017 May 2]. <http://www.teamtextiles.com/>.

12. Kevlar 49. Seguin (TX): Hexcel; 2014 June [accessed 2017 May 3].
http://www.hexcel.com/user_area/content_media/raw/HRH_49_us.pdf.
13. Polyurethane adhesive films. Pine Brook (NJ): Adhesives Films, Inc.; c2013 [accessed 2017 May 2].
http://www.adhesivefilms.com/Polyurethane__UAF_Series.html.
14. Boyd SE, Wolbert JP. Multi-impact durability and processing of thick-section carbon-glass/epoxy hybrid composites toughened with thermoplastic polyurethane inter-layer films. Aberdeen Proving Ground (MD): Army Research Laboratory (US); 2012 Sep. Report No.: ARL-TN-0501.
15. Boyd SE, Emerson RP, Bogetti TA. Low-velocity, multi-impact durability performance of thick-section 3WEAVE S2-glass/SC-15 composites toughened with thermoplastic polyurethane inter-layer films. Aberdeen Proving Ground (MD): Army Research Laboratory (US); 2013 Aug. Report No.: ARL-TR-6547.
16. Alfredsson KS, Bogetti TA, Carlsson LA, Gillespie JW Jr, Yiournas A. Flexure of beams with an interlayer: symmetric beams with orthotropic adherends. *J Mechanics of Materials and Structures*. 2008;3(1):45–62.
17. Emerson RP, Cain J, Simeoni M, Lawrence B. Processing and evaluation of 3D-reinforced needled composite laminate. Aberdeen Proving Ground (MD): Army Research Laboratory (US); Sep 2012. Report No.: ARL-TR-6107.
18. Emerson RP, Lawrence B, Montgomery A, Safriet S. Improvements to the processing and characterization of needled composite laminates. Aberdeen Proving Ground (MD): Army Research Laboratory (US); 2014 Jan. Report No.: ARL-RP-472.
19. ASTM D 7136. Standard test method for measuring the damage resistance of a fiber-reinforced polymer matrix composite to a drop-weight impact event. West Conshohocken (PA): ASTM International; 2015.
20. ASTM D 7137. Test method for compressive residual strength properties of damaged polymer matrix composite plates. West Conshohocken (PA): ASTM International; 2012.
21. ASTM D 7264. Standard test method for flexural properties of polymer matrix composite materials. West Conshohocken (PA): ASTM International; 2015.
22. ASTM D 2344. Standard test method for short-beam strength of polymer matrix composite materials and their laminates. West Conshohocken (PA): ASTM International; 2016.

23. ImageJ: Image processing and analysis in Java. nd [accessed 2017 May 2].
<https://imagej.nih.gov/ij/>.

List of Symbols, Abbreviations, and Acronyms

2-D	2-dimensional
3-D	3-dimensional
3PB	3-point bend
CAI	compression after impact
CI	compliant interlayer
CoV	coefficient of variation
PRSEUS	Pultruded Rod Stitched Efficient Unitized Structure
SBS	short-beam shear
TPU	thermoplastic polyurethane
VARTM	vacuum-assisted resin transfer molding
XLADD	Extremely Lightweight, Adaptive, Durable, and Damage Tolerant

1 DEFENSE TECHNICAL
(PDF) INFORMATION CTR
DTIC OCA

2 DIRECTOR
(PDF) US ARMY RESEARCH LAB
RDRL CIO L
IMAL HRA MAIL & RECORDS
MGMT

1 GOVT PRINTG OFC
(PDF) A MALHOTRA

2 DIR USARL
(PDF) RDRL VTM
R HAYNES
RDRL WMM A
S BOYD